

CHANGES OF WELD POOL SHAPE BY VARIATIONS IN
THE DISTRIBUTION OF HEAT SOURCE IN ARC WELDING

N. S. Tsai & T. W. Eagar

Department of Materials Science and Engineering
Massachusetts Institute of Technology
Cambridge, MA 02139
USA

Summary

Weld width, penetration, and cross-sectional area were presented as a function of heat input and arc heat distribution parameter in dimensionless forms. The theory was based on a closed form solution to a travelling gaussian heat source. The gaussian heat distributions were determined by measuring actual heat distributions in arcs on a water-cooled copper anode. The results indicate both welding process parameters (current, arc length, travel speed) and material parameters have significant effects on weld pool shape. The prediction was compared with experimental results with generally good agreement.

List of Symbols

a	=	thermal diffusivity
c	=	specific heat
k	=	thermal conductivity
n	=	operating parameter ($n = qv/4\pi a^2 \rho [T_c - T_0]$)
q	=	net heat input per unit time (power)
Q	=	power distribution
R	=	distance to the center of arc ($R = (w^2 + y^2 + z^2)^{1/2}$)
R*	=	dimensionless distance from the center of the arc ($R* = [\xi^2 + \psi^2 + \zeta^2]^{1/2}$)
T	=	temperature
T ₀	=	initial temperature
T _c	=	critical temperature
u	=	dimensionless distribution parameter ($u = v\sigma/2a$)
v	=	travel speed of arc
w	=	distance in x direction in a moving coordinate of speed v ($w = x - vt$)
y	=	distance in y direction
z	=	distance in z direction
σ	=	distribution parameter
ρ	=	density
δQ	=	incremental amount of heat
τ	=	dimensionless time
θ	=	dimensionless temperature ($\theta = [T - T_0]/[T_c - T_0]$)
ξ	=	dimensionless distance in the moving coordinate ($\xi = vw/2a$)

ψ = dimensionless distance y
 ζ = dimensionless distance z

Introduction

It has been more than forty years since Rosenthal presented his solution of a travelling point source of heat [1] which has been the basis for most subsequent studies of heat flow in welding. Christensen put the results in dimensionless form in order to demonstrate that the solution applies to many materials over wide ranges of heat input [2]. Since that time a number of refinements have been offered [3-6]. Several have attempted to use a more realistic distributed heat source [3,4,6], but none have solved the entire temperature field for a travelling distributed source. More recently, a general form of the travelling distributed heat source has been offered, but calculations of the thermal field were limited and unexplained [7].

As pointed out by Rykalin [3], a heat flow model needs to take the following factors into consideration:

- non-constant thermal properties
- heat of phase transformation
- heat input magnitude and distribution
- plate geometry
- convection and surface depression in weld pool [8].

Although Christensen's experimental results indicate that the Rosenthal solution gives good agreement with the actual weld bead size over several orders of magnitude, the scatter can be as much as a factor of three. The work of Grosh [9] showed that the effect of non-constant thermal property can only make a 10-15 percent difference in the weld pool geometry, and Malmuth [5] has shown that the effect of latent heat can only make a 5-10 percent difference. Obviously, the heat input magnitude solution of Rosenthal modified for non-constant thermal properties and latent heat cannot explain the difference between theoretically predicted and experimentally measured importance of the heat distribution on the plate surface. Fortunately, several investigators have measured actual heat distributions in arcs on a water-cooled copper anode [10,11,12]. Using these results, it is possible to determine whether the presence of a distributed rather than a point source of heat can explain the range of weld shape variation measured by Christensen and others.

It should be emphasized that this solution retains all but one of the simplifying assumptions used by Rosenthal including absence of convection in weld pool, constant thermal property, and no latent heat of phase transformation. The only change is the use of a distributed rather than a point source of heat. In spite of these simplifications, it will be shown that the results not only agree with the Rosenthal solution in the limit, but that they are capable of explaining most of the experimental scatter.

Formation of the Solution

Rosenthal's solution for the temperature distribution produced by a travelling point heat source was converted to dimensionless form by Christensen [2]:

$$\theta = n \frac{e^{-(\xi + R^*)}}{R^*} \quad (1)$$

where the operating parameter, n , includes the heat input, the travel speed, and the thermal diffusivity of the workpiece.

The solution for a gaussian heat source travelling on the surface of a semi-infinite plate as shown in Figure 1 can be formulated as follows: The gaussian heat source, Q , as shown in Figure 2, is defined by the magnitude, q , and the distribution, σ . The heat distribution, Q , is given by

$$Q(x,y) = \frac{q}{2\pi\sigma^2} e^{-(x^2 + y^2)/2\sigma^2} \quad (2)$$

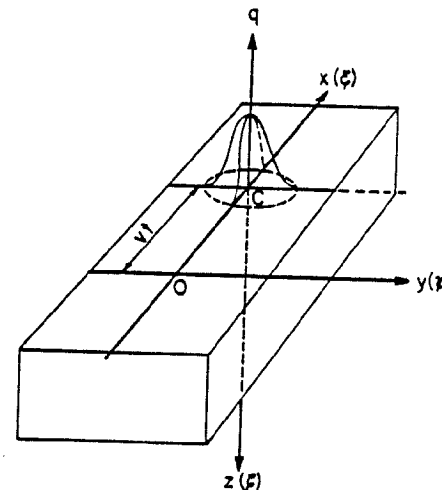


Figure 1 - A gaussian distributed heat source moving on the surface of a semi-infinite plate, and (ξ, ψ, ζ) are the dimensionless distances from the center of the arc in a coordinate moving at speed, v , in the x direction.

The heat conduction equation is solved first in a fixed coordinate using an instantaneous gaussian heat source. It is then integrated with respect to time in a moving coordinate to provide a quasi-steady state travelling solution. The temperature rise for a point of heat, δQ , in a very small amount of time given by [13]:

$$dT_t' = \frac{\delta Q dt'}{\rho c [4\pi a (t - t')]^{3/2}} e^{-\frac{(x - x')^2 + (y - y')^2 + (z - z')^2}{4a(t - t')}} \quad (3)$$

where δQ is the amount of heat located at position (x', y', z') at time t' . The solution of an instantaneous gaussian heat source is the super position of a series of point heat source solutions over the distributed region. By substituting the gaussian distributed heat source for the point heat source δQ , this superposition is performed by the integration

$$dT_{t'} = \int_{-\infty}^{\infty} dx' \int_{-\infty}^{\infty} dy' \frac{q e^{-(x'^2 + y'^2)/2\sigma^2}}{2\pi\sigma^2} \frac{dt'}{\rho c [4a(t-t')]^{3/2}}$$

$$e^{-\frac{(x-x')^2 + (y-y')^2 + (z-z')^2}{4a(t-t')}} =$$

$$\frac{[q dt'] \exp\left[-\frac{x^2 + y^2}{4a(t-t')} + \frac{z^2}{4a(t-t')}\right]}{2\pi\sigma c [4\pi a(t-t')]^{1/2} [2a(t-t') + \sigma^2]} \quad (4)$$

This corresponds to the rise of temperature during a very short time interval from time, t' , to $t'+dt'$ due to an amount of gaussian heat $q dt'$ released on the surface.

When considering the gaussian heat source travelling with a constant speed v , the total increase of temperature is the sum of all contributions in the time interval from $t'=0$ to $t'=t$. A simpler expression of the solution is expected if the solution is presented in a moving coordinate system with travel speed v . This summation can be carried out again by integration.

$$T - T_0 = \int_{t'=0}^{t'=t} dT_{t'}$$

$$= \frac{q}{\rho c (4\pi a)^{1/2}} \int_0^t \frac{dt' (t-t')^{-1/2}}{2a(t-t') + \sigma^2} e^{-\frac{(x-vt')^2 + y^2}{4a(t-t')} - \frac{z^2}{4a(t-t')}} \quad (5)$$

For simplicity, let $t''=t-t'$, then $dt''=-dt'$ and $x-vt'=w+vt''$, where $w=x-vt$. Eq. 9 can be written as

$$T - T_0 = \int_0^t dt'' \frac{q}{\rho c (4\pi a)^{1/2}} \frac{t''^{-1/2}}{2at'' + \sigma^2} e^{-\frac{w^2 + y^2 + 2wvt'' + v^2 t''^2}{4at'' + 2\sigma^2} - \frac{z^2}{4at''}} \quad (6)$$

This is the solution of the temperature distribution for a gaussian distributed heat source moving on a semi-infinite plate with no change in phase.

The solution may be put in dimensionless form by using the following dimensionless variables:

$$\xi = vw/2a, \quad \psi = vy/2a, \quad \zeta = vz/2a, \quad \tau = v^2 t''/2a, \quad \text{and } u = v\sigma/2a$$

Eq. 6 then reduces to

$$\theta = \frac{n}{\sqrt{2\pi}} \int_0^{\frac{v^2 t}{2a}} d\tau \frac{\tau^{-1/2}}{\tau + u^2} e^{-\frac{\xi^2 + \psi^2 + 2\xi\tau + \tau^2}{2\tau + 2u^2} - \frac{\zeta^2}{2\tau}} \quad (7)$$

Further solution of this equation requires a numerical procedure. This solution can be reduced to the Rosenthal equation in the limit of a point heat source. By requiring $u = 0$, Eq. 7 is reduced to Eq. 1.

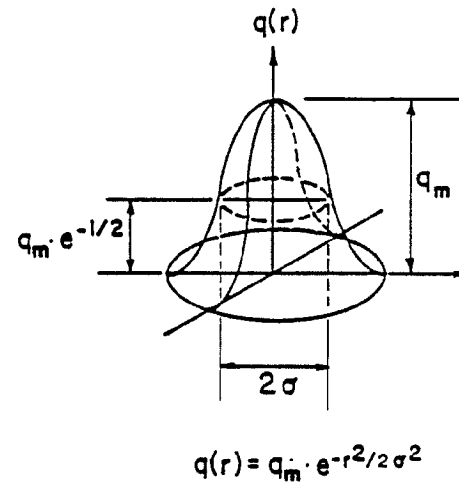


Figure 2 - Gaussian distribution function: Distribution, σ , is defined as the standard deviation of the gaussian function.

Results and Discussion

Results of the Model

In order to present the solution of Eq. 7, it is necessary to know the value of the distribution parameter, σ . Nestor (10), Schoeck (11), and Tsai (12) have measured the heat distributions of arcs on water-cooled anodes. Although the measured distributions are not true gaussians, the

results can be approximated as gaussians by a least squares regression, subject to the constraint that the total area under the experimental and the gaussian curves are equal. This produces a gaussian distribution of equal total heat input as the experimental distribution.

Figure 3 shows the distribution parameter, σ , as a function of current and arc length. The distribution parameter, σ , increases both with arc length and current. It is also important to know the typical values of operating parameter, n , and dimensionless distribution parameter, u . Typical values of n and u for gas tungsten arc welding on carbon steel are shown in Table 1. A travel speed of 2.5mm/sec. and a distribution parameter of 2.4mm will give a dimensionless distribution parameter, u , of 0.6 and an operating parameter, n , of .7.

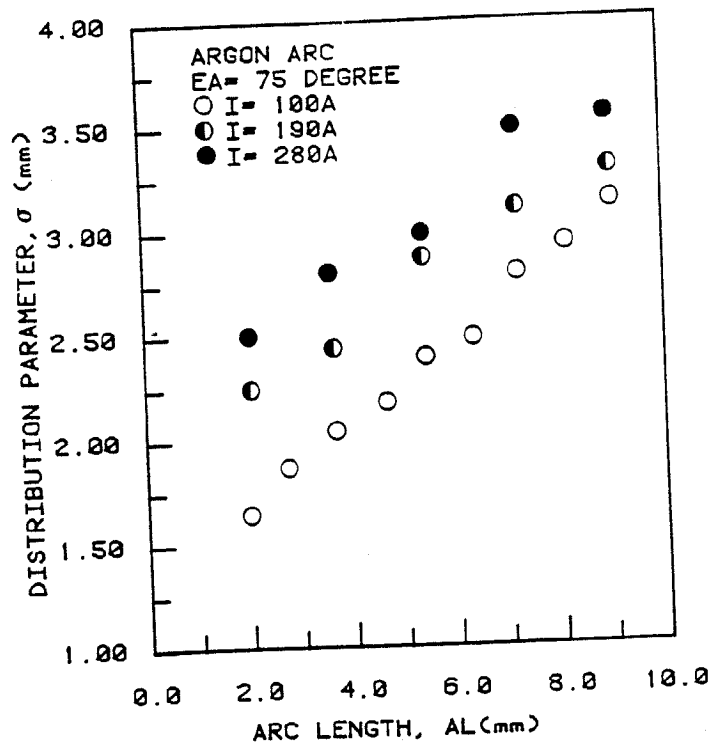


Figure 3 - Distribution parameter, σ , is a function of arc length and current.

Figures 4 and 5 show the width and depth of the weld pool. As a function of the operating parameter, n , Figure 4 shows that at low n , which corresponds to low heat input, the weld width is less than the Rosenthal solution, but as n increases, the width rapidly increases to greater than the Rosenthal solution. Figure 5 shows that the weld depth always remains less than the Rosenthal solution.

Table I - Typical Values of Operating Parameter, n , and Dimensionless Distribution Parameter, u .

Distribution Parameter	(mm)	2.4
Thermal Conductivity	$k(w/cmK)$	0.33
Heat Capacity	$\rho c(J/cm^3K)$	5.4
Thermal Diffusivity	$a(cm^2/sec)$	0.05
Travel Speed	$v(cm/sec)$	0.25
Current	$I(amps)$	100
Voltage	$V(volts)$	12
Arc Efficiency	η	0.6
Heat Input	$q(KW)$	0.72
Operating Parameter	n	0.7
Dimensionless Distribution Parameter	u	.6

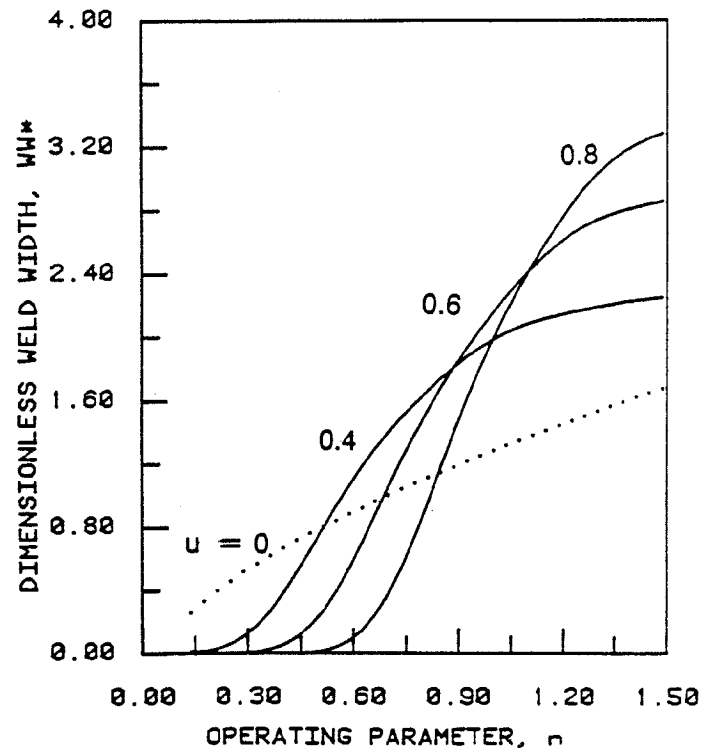


Figure 4 - WW* versus n : Dimensionless weld width WW* versus operating parameter, n , as a function of dimensionless distribution of parameter, u .

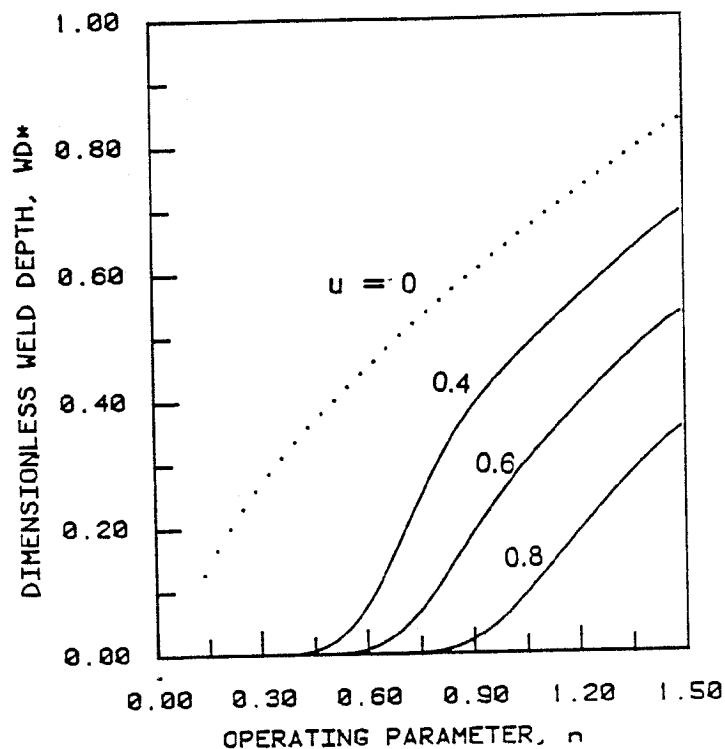


Figure 5 - WD^* versus n : Dimensionless weld depth WD^* versus operating parameter, n , as a function of the dimensionless distribution parameter, u .

The result is consistent with the work of Glickstein (14). He measured changes in weld width with arc length at constant heat input. Similar tests made in our laboratory are shown in Figure 6. At low heat inputs the weld width decreases with increasing arc length. A physical explanation for these results is that at low heat input a broader heat distribution will produce a narrow weld because there is not sufficient heat to cause melting. However, at high heat input, there is always sufficient heat to cause melting. A broader heat distribution will produce a greater weld width. At a heat input between 500J/mm and 750J/mm the slope of width versus arc length changes from negative to positive. This transition region corresponds to the crossover region of Figure 4.

Figure 7 shows the depth to width ratio as a function of operating parameter, n . The ratio varies from 0 to .3 which is consistent with most ratios which have been reported in the literature (15). Nonetheless, recent results show that under some conditions convection may have a strong influence on weld pool shape (16). As noted previously, convection is not considered in the solution presented here, yet under many circumstances the pure convection model presented here is reasonable accurate.

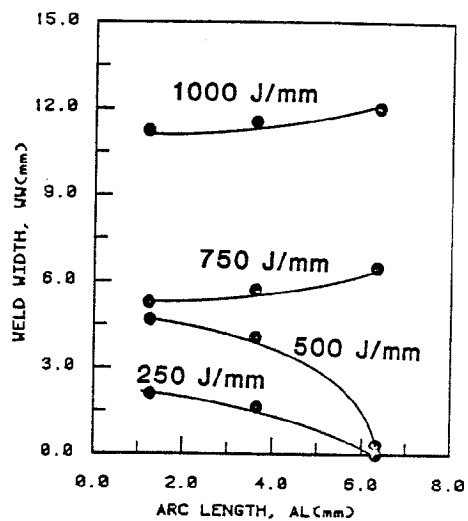


Figure 6 - W versus arc length: Experimental weld width versus arc length as a function of heat input per unit length.

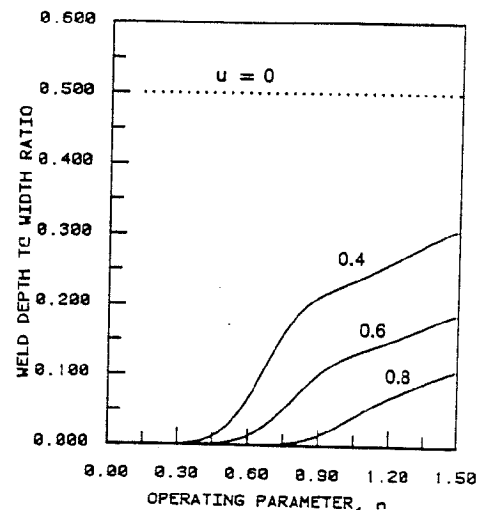


Figure 7 - WD^*/WW^* versus n : Calculated depth to width ratio versus operating parameter, n , as a function of the dimensionless distribution parameter, u , equal to 0, 0.4, 0.6 and 0.8.

Figure 8 gives the weld cross sectional area. This is made by complete solution of Eq. 7 in two dimensions. It is seen that the area deviates significantly from the Rosenthal solution depending on the distribution of the heat source.

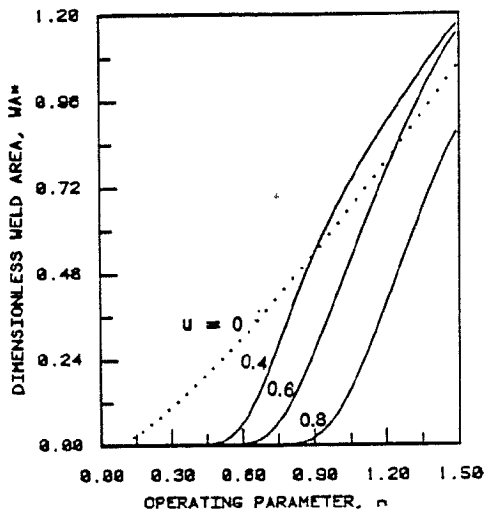


Figure 8 - Dimensionless area of the weld metal, WA^* , versus operating parameter, n , as a function of the dimensionless distribution parameter, u .

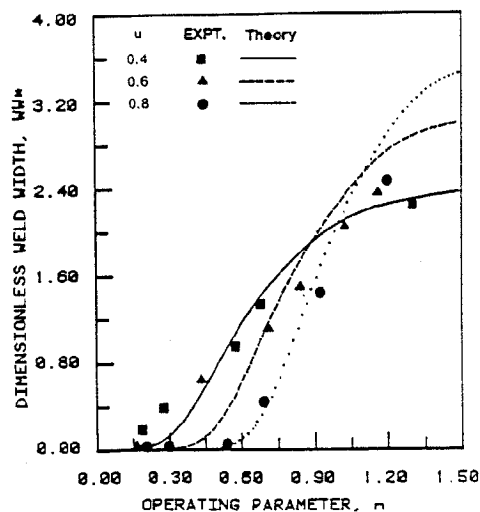


Figure 9 - Distributed source solution is in good agreement with experimental data.

The accuracy of this model was tested using three levels of heat distribution. Changes in the process parameters such as current and voltage were correlated with changes in heat distribution on the surface of a water-cooled anode. The experimental weld width as a function of n and u are in good agreement with the theory as shown in Figure 9.

Conclusions

The travelling distributed heat source theory provides the first a priori estimates of weld pool geometry based upon fundamentals of heat transfer. Although a number of simplifying assumptions remain, the agreement between theory and experiment is improved considerably over previous models; however, the greatest value of this work does not lie in the ability to predict the absolute size of the weld zone. Rather, the strength of this new theory is that it gives an accurate functional relationship between both process parameters and materials parameters. The theory provides a model which can be used to assess how changes in the process or in the material will influence the weld geometry. Such a model is essential to many automation and control strategies now being considered for welding processes.

Acknowledgements

The authors wish to express their appreciation to Prof. Nils Christensen for several helpful discussions. They are grateful for financial support from the Department of Energy under contract DE-AC02-78ER 94799 A.0003.

References

- Rosenthal, D., "The Theory of Moving Source of Heat and its Application to Metal Transfer," Transactions ASME, 43(11)(1946) pp. 849-866.
- Christensen, N., Davies, V. and Gjermundsen, K., "The Distribution of Temperature in Arc Welding," British Welding Journal, 12(2) (1965) pp. 54-75.
- Rykalin, N. N., and Nikolaev, A. V., "Welding Arc Heat Flow," Welding in the World, 9(3/4)(1971) pp. 112-132.
- Ravelic, V., "Weld Puddle Shape and Size Correlation in a Metal Plate Welded by the GTA Process," pp. 251-258 in Arc Physics and Weld Pool Behavior, The Welding Institute Conference, London, 1979.
- Malmuth, N. D., Hall, W. F., Davis, B. I., and Rosen, C. D., "Transient Thermal Phenomena and Weld Geometry in GTAW," Welding Journal 53(9) (1974) pp. 388s.
- Friedman, E., "Thermodynamic Analysis of the Welding Process Using the Finite Element Method," ASTM Transactions, Journal of Pressure Vessel Technology, (7)(1975) pp. 206.
- Peng, T. C., Sastry, S. M. L., and O'Neal, J. E. "Exploratory Study of Laser Processing of Titanium Alloys," pp. 279-292 in Lasers in Metallurgy, the Metallurgical Society of AIME, 1981.

8. Lin, M. L., "Influence of Surface Depression and Convection on Weld Pool Geometry," Masters Thesis, Massachusetts Institute of Technology, Cambridge, MA, 1982.
9. Grosh, R. J., Trabant, E. A., "Arc Welding Temperature," Welding Journal, 35(8)(1956) pp. 396s-400s.
10. Nestor, O. H., "Heat Intensity and Current Density Distribution at the Anode of High Current Inert Gas Arcs," Journal of Applied Physics, 33(5)(1967) pp. 1638-1648.
11. Shoock, P., "An Investigation of Anode Energy Balance of High Intensity Arcs in Argon," pp. 353-478 in Modern Development of Heat Transfer, Academic Press, New York, 1963.
12. Tsai, N. S. and Eagar, T. W., "Variation of the Heat Distribution with Welding Parameters in Gas Tungsten Arc Welding," to be published.
13. Carslaw, H. S. and Jaeger, J. C., Conduction of Heat in Solid, p. 255; Oxford University Press, 1967.
14. Glickstein, S. S., Friedman- E., and Yeniscavich, W., "An Investigation of Alloy 600 Welding Parameters," Welding Journal, 54(4)(1975) pp. 113s-122s.
15. Glickstein, S. S., and Yeniscavich, W., "Review of Minor Element Effects on the Welding Arc and Weld Penetration," Welding Research Council Bulletin, 266(1977) p. 18.
16. Heiple, C. R., and Roper, J. R., "Effect of Selenium on GTAW Fusion Zone Geometry," Welding Journal, 60(8)(1981) pp. 143s-145s.